Decoherence effects in the dynamics of interacting ultracold bosons in disordered lattices

Benoît Vermersch, Jean-Claude Garreau

Decoherence effects in the dynamics of interacting ultracold bosons in disordered lattices

Benoît Vermersch and Jean Claude Garreau[a]

Laboratoire de Physique des Lasers, Atomes et Molécules, Université Lille 1 Sciences et Technologies, CNRS; F-59655 Villeneuve d'Ascq Cedex, France

Abstract We study the interplay between disorder, interactions and decoherence induced by spontaneous emission process. Interactions are included in the Anderson model via a mean-field approximation, and a simple model for spontaneous emission is introduced. Numerical simulations allow us to study the effects of decoherence on different dynamical regimes. Physical pictures for the mechanisms at play are discussed and provide simple interpretations. Finally, we discuss the validity of scaling laws on the initial state width.

1 Introduction

The Anderson model [1], is a simple, tractable, model describing disorder effects on electrons in a crystal. The model predicts that in disordered crystals the eigenfunctions may become spatially localised [1], in sharp contrast with the Bloch functions of a perfect crystal, a phenomenon called *Anderson localisation*. However, due to its very simplicity, the model (in its original form) overlooks potentially important effects: It is a single particle, zero temperature model.

Recently, analogs of the Anderson model have been realized with cold or ultracold atoms, which can be made much closer to the Anderson model than a crystal. A direct translation of the Anderson model can be obtained by placing ultracold atoms in a far-detuned laser speckle, which realizes a random mechanical potential affecting the center-of-mass of the atom, and allowed observation of the localisation in one dimension (1D) with bosons [2,3]. The 3D localisation was also studied with both fermions [4] and bosons [5]. The quasiperiodic kicked rotor can also realize an equivalent of both 1D [6,7,8] and 3D systems [9,10]; the latter allowing a detailed experimental study of the Anderson *transition*, including measurements of the critical wavefunction [11] and of its critical exponent [10,12,13]. Ultracold atom systems allow a large control of decoherence, which is essentially due to spontaneous emission, and of atom-atom interactions, for which an experimental "knob" is provided by the Feshbach resonances [14], making them an ideal tool for studies of the interplay of quantum effects, disorder, interactions, and decoherence.

---

[a] http://www.phlam.univ-lille1.fr/atfr/cq

[1] In 1D all eigenfunctions are localised, in 3D an energy "mobility edge" separates localised from delocalised ones.

We have recently studied numerically and theoretically the influence of interactions in a bosonic 1D Anderson system [15], which is a very active research domain [16,17]. The sensitivity of the system to the initial state was shown to be characterised by a scaling law *depending on the initial state*. In the present paper we introduce the effect of decoherence due to spontaneous emission in the problem, and show that Anderson localisation (AL) is promptly destroyed by it, but the resulting dynamics still respects the scaling law mentioned above. This confirms the pertinence of the scaling strategy, and indicates that it is a relevant approach for studying disordered interacting systems.

2 The model

We essentially use in the present paper the same model as in [15], except for the introduction of decoherence effects as discussed below. Briefly, we start with a gas of interacting bosons evolving in the sinusoidal potential formed by a 1D standing wave $V(x) = -V_0 \cos^2(k_L x)$. In the mean field approximation, the ultracold gas can be represented by a single wave-function $\psi_\epsilon(x)$ obeying the Gross-Pitaesvkii equation (GPE):

$$i\hbar\dot{\psi}_\epsilon(x) = \left(\frac{p^2}{2m} + V(x) + g|\psi_\epsilon(x)|^2\right)\psi_\epsilon(x)$$

Projecting the solution on a basis of localised Wannier functions $w_n(x)$, $\psi_\varepsilon(x) = \sum_n c_n(t)w_n(x)$ leads to the well-known *tight-binding* description:

$$i\hbar\dot{c}_n = v_n c_n - t_{n-1}c_{n-1} - t_{n+1}c_{n+1} + g\left|c_n\right|^2 c_n, \tag{1}$$

where g represents the interaction strength which is proportionnal to the s-wave scattering length, and we kept only nearest-neighbors hopping terms, i.e. $t_{n+m} = 0$ if $|m| > 1$. According to standard conventions, the hopping term is symmetric $t_{n+1} = t_{n-1} = T$ and we measure energies in units of T and time in units of $\hbar/T$. Following the Anderson "recipe" [1] we introduce "diagonal" disorder by randomizing the onsite energies v_n in an interval $[-W/2, W/2]$; each choice of an ensemble $\{v_n\}$ producing a "realization" of the disorder, so, finally:

$$i\dot{c}_n = v_n c_n - c_{n-1} - c_{n+1} + g\left|c_n\right|^2 c_n. \tag{2}$$

As we use mean field theory throughout this work, we shall use the terms "interaction" and "nonlinearity" interchangeably.

Spontaneous emission (SE) is inevitably – although controllable – present in an optical potential. For a laser-atom detuning $\Delta = \omega_L - \omega_0 \gg \Gamma_0$ (where ω_L is the laser frequency and ω_0 the atomic transition frequency and Γ_0 the natural width of the transition) the amplitude V_0 of the potential is $V_0 = \hbar\Omega^2/8\Delta$, where Ω is the resonance Rabi frequency. The SE ratio is then given by

$$\Gamma_{\rm se} = \frac{\Gamma_0}{4}\frac{\Omega^2}{\Delta^2 + \Omega^2/2 + \Gamma_0^2/4} \sim \frac{\Gamma_0\Omega^2}{4\Delta^2}$$

where the approximate expression corresponds to the large-detuning limit $|\Delta| \gg \Gamma_0, \Omega$. For common parameters used in experimental setups, $\Gamma_{\rm se} \lesssim 10{\rm s}^{-1}$, $T/\hbar \sim 1000{\rm s}^{-1}$ so that in our rescaled units, the spontaneous emission rate γ in reduced units is typically $\gamma \lesssim 10^{-2}$.

We model the effect of spontaneous emission by a Monte Carlo procedure simulating spontaneous emission events according to the probability γ. If a SE event

happens, as we are considering a one-dimensional lattice, we simply translate the momentum p *of the condensate* (i.e. the order parameter Fourier transform $\psi(p)$) by a vector $\hbar k_L \cos\theta$, or, in reduced units $\pi \cos\theta$, with θ being a randomly picked angle (in the interval $[0, 2\pi]$) representing the direction of the emitted photon with respect to the direction of the laser beam. Between two spontaneous emission events, the evolution of c_n is calculated from Eq. (2). This way of modeling SE has been often used for *individual atoms* in optical lattices [18,13,19] and compares very well with experimental signals. It can however be asked if it can also be applied to the *condensate* wavefunction in the mean-field approximation. This can be justified, at least for low SE rates, by the following argument. In a condensate, a photon can be absorbed in two ways: either an individual atom aborbs it and goes to an excited state, or it is absorbed collectivelly generating a "delocalised" excitation. In the former case, the individual atom is not anymore on the condensate and does not contribute to the mean-field dynamics described by the Gross-Pitaevskii equation; in the latter case there is no changing in the condensate population and it is reasonable to consider that it is the *collective* mean-field wavefunction that "recoils" to compensate the photon momentum [2]. Our model of the spontaneous emission corresponds to a collective recoil of the condensate wavefunction (and to a progressive increasing of the non-condensate fraction which is not taken into account) an approximation which is valid as long as this fraction stays small, that is, for low SE rates compared to the duration of the experiment.

As in ref. [15], we work with a system of fixed size of L sites, with absorbing boundaries to prevent wavepacket reflections. This is done by setting a slowly varying imaginary potential at the edges of the box. The wavepacket is thus depleted if it is (or becomes) large enough to touch the borders of the box, and the survival probability p is the integral of the wavepacket still present inside the box at time t:

$$p(g,t) = \sum_{n=-L/2}^{L/2} |c_n(t)|^2 .$$

A diffusive dynamics is thus characterised by a continuous decrease of $p(g,t)$ with t. In the present work typically $L = 101$ sites.

In presence of interactions, the system is nonlinear and thus sensitive to the initial state. In order to characterise the resulting dependence of the dynamics on the size of the initial state, we study a particular family of initial states of square shape and width L_0:

$$c_n(0) = \begin{cases} L_0^{-1/2} & \exp\left[i\theta_n\right], \ |n| \leq (L_0-1)/2 \\ 0 & \text{otherwise.} \end{cases} \tag{3}$$

with *random* phases θ_n (for a discussion of the consequences of this choice, see [15]).

3 Decoherence effects in disordered, interacting systems

In a tight-binding approach, one associates eigenenergies and eigenstates to lattice sites. In a periodic lattice, each eigenenergy matches a degenerate correspondant in a neighbor site, which allows tunneling and diffusion. In presence of diagonal disorder, this degeneracy is removed, and only *virtual* tunneling is allowed, which leads to the exponentially localised Anderson eigenstates. However, spontaneous emission can couple Anderson eigenstates even if they are not degenrate, and thus induces diffusive motion in a disordered lattice.

---

[2] This process is somewhat analogous to what happens in the Mossbaeur effect.
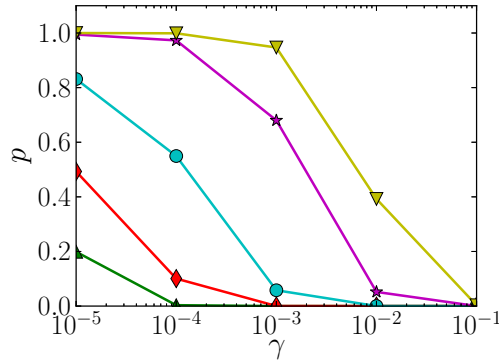
Figure 1. (Color online) Survival probability p as a function of the spontaneous emission rate γ at $t = 10^5$ in the absence of interactions ($g = 0$). Values of the disorder W are 2 (green triangles), 3 (red diamonds), 4 (cyan circles) , 6 (magenta stars) and 8 (yellow inverted triangles). The width of the initial state is $L_0 = 21$.

Figure 1 shows the survival probability p at time $t = 10^5$ as a function of the spontaneous emission rate γ for five values of the disorder W, in absence of interactions ($g = 0$). Data were averaged over a total of 500 realizations of the disorder $\{v_n\}$, of the inital phase distribution $\{\theta_n\}$ and of SE emission times. At time t, there have been on the average γt spontaneous emission events. The number of spontaneous emission events necessary for destroying AL depends on the disorder W. For $W = 2$ (green triangles), 10 spontaneous emissions are enough to induce complete diffusion of the wavepacket whereas for $W = 8$ (yellow inverted triangles) the wavepacket escapes from the box after 10^4 events ($\gamma = 10^{-1}$).

One can interpret these results in two equivalent ways. A "static" point of view consists on noting that the initial state [Eq. (3)], due to the choice of random phases, projects over *all* Anderson eigenvalues. These eigenstates have different localisation lengths, with a maximum at the center of the band given by $\ell_0 \sim 96 W^{-2}$ [20], and zero at the borders of the band. If the disorder is small, a typical Anderson eigenstate has width comparable or larger than the box width $L = 101$, it is thus absorbed in a short time. The initial survival probability then corresponds to the fraction of Anderson eigenstates with localisation length much smaller that L. However, when a spontaneous emission event happens, it *redistributes* the quantum phases, and projects again a part of the wavepacket on eigenstates that are either very large or centered in positions close to the border of the box, which are then absorbed, and this repeated process progressively leads to the destruction of the AL. A dynamic point of view considers that the initial state evolves during a characteristic localisation time $t_{\mathrm{loc}} \sim W^{-2}$ until it localises, with a typical width $\langle x^2 \rangle \sim W^{-4}$. The phase redistribution due to a spontaneous emission event breaks the quantum interference responsible for the localisation, diffusion starts again for a time t_{loc}, and then stops until the next SE event, and so on. For low SE ratios $\gamma t_{\mathrm{loc}} \leq 1$, if D is the disordered-averaged *classical* diffusion coefficient, then one can estimate the diffusion coefficient induced by SE as $D_{\mathrm{SE}} = D t_{\mathrm{loc}} \gamma$.

Figure 2 presents spatial probability distributions $|c_n|^2$ for $t = 10^5$, $W = 4$, $L_0 = 3$ for various values of the spontaneous emission rate γ. For $\gamma = 0$ (blue solid line) this distribution is exponentially localised $|c_n|^2 \propto \exp\left(-2 |n| / \ell\right)$, where ℓ is the localisation length, comparable to $\ell_0(W)$, the maximum localisation length of the Anderson eigenstates. For $\gamma = 10^{-5}$ (green dotted line), the system is only weakly affected by
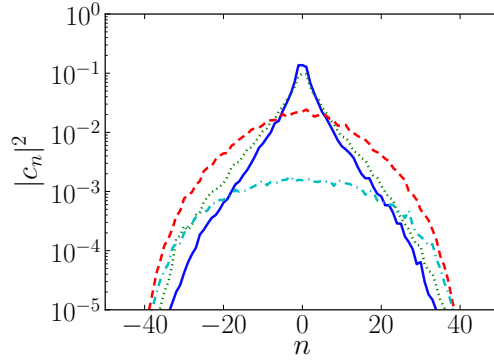
Figure 2. (Color online) Density distribution $|c_n|^2 (t = 10^5)$ *vs* site index n, for $g = 0$, $W = 4$, $L_0 = 3$. Values of γ are: 0 (blue solid line), 10^{-5} (green dotted line), 10^{-4} (red dashed line) and 10^{-3} (dot-dashed cyan line). Anderson localisation, characterised by the exponential (triangular in logarithmic scale) shape is progressively destroyed when decoherence increases.

spontaneous emission (as just one event happens in average during the time evolution), a small diffusion is observed in the tails of the distribution. For $\gamma = 10^{-4}$ (red dashed line) and $\gamma = 10^{-3}$ (dot-dashed cyan line), the distribution has taken a Gaussian shape, indicating that the decoherence-induced diffusion has become dominant. Alternatively, this process can be interpreted "statically" as a phase reshuffling provoked by spontaneous emission, which excites eigenstates centered everywhere in the box L, so that the localisation length is not anymore a relevant length scale in the problem.

Consider now the repulsive interacting case ($g > 0$). It is useful, if not completely rigorous, to interpret the nonlinear term in Eq. (2), as a *dynamical perturbation* $v^{\mathrm{NL}} \equiv g|c_n|^2$ of the on-site energy v_n, depending on the population of the site. For $v^{NL} \ll W$ – which implies a low-density, spatially extended, wavepacket – Anderson localisation is expected to survive for a very long time: Anderson eigenstates whose localisation length ℓ is inferior to the size of the box remain in the system and give non-zero survival probability. For $v^{\mathrm{NL}} \sim W$, if the $c_n(t)$ vary rapidly, the dynamical correction can bring temporarily neighbour levels close to degeneracy, restablishing transport. This mechanism is most efficient in the so-called *chaotic regime*, where the $c_n(t)$ display a stochastic character. If $v^{\mathrm{NL}} \gg W$, neighbour sites are decoupled from each other even for small population differences, which leads to a different, nonlinear, type of localisation called *self-trapping*, favored for narrow (small L_0) initial states. Figure 3 displays the survival probability $p(t = 10^5)$ as a function of the interacting strength g, for $W = 4$ and four values of the decoherence level γ from 0 to 10^{-3}. The three dynamical regimes are clearly visible, a plateau for small values of g due to surviving AL, a dip created by the chaotic diffusion for intermediate values of g, and a reduction of diffusion due to self-trapping for high values of g, leading to a complete freezing for $g \approx 300$. Clearly, the three dynamical regimes are not affected in the same way by decoherence: Anderson localisation, which relies on delicate phase relations is more sensitive to decoherence. Comparison of the curves for $\gamma = 0$ (solid blue) and $\gamma = 10^{-5}$ (dotted green) shows that even *one* SE event in the average has an observable effect on AL. In the chaotic regime, the diffusion due to chaotic motion and diffusion due to decoherence tend to add to each other, but a strong diffusion due to decoherence decreases the site populations, and thus the nonlinear term $g \sum_n |c_n|^2$. This effect of dilution due to decoherence explains the fact that the frontier between
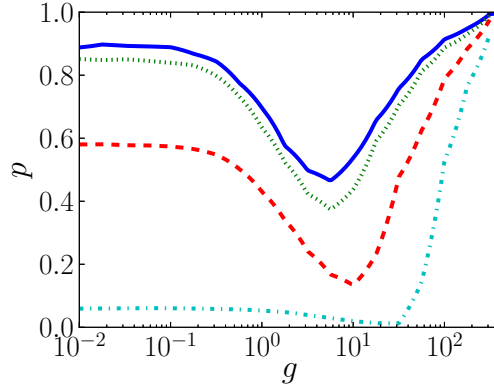
Figure 3. (Color online) Survival probability p as a function of the interacting strength g for $t = 10^5$. Values of γ: 0 (blue solid line), 10^{-5} (green dotted line), 10^{-4} (red dashed line) and $\gamma = 10^{-3}$ (dot-dashed cyan line). Three dynamical regimes are clearly visible: Localized (low g), chaotic (intermediate values of g), and self-trapped (high g). Other parameters are $W = 4$ and $L_0 = 3$.

the various regimes is shifted to higher values of g when γ increases. Self-trapping, not relying on quantum inteference, but only on populations $|c_n|^2$ (which are not directly affected by SE) tends to be insensitive to decoherence: for $g \approx 320$ all curves converge to unitary survival probability.

Figure 4 shows spatial distributions at $t = 10^5$ for $g = 10$ (a) and $g = 320$ (b). In the chaotic regime (a) and for low decoherence rate (solid blue, dotted green lines), the wavepacket has its exponential shape preserved in the center of the box but non-exponential tails appear. This is due to the fact that interactions depopulate the center of the box (where populations and thus nonlinearity is maximum), but it preserves the exponential shape [15]. The question whether Anderson localisation is destroyed in this case is tricky: The wavepacket spreads along the box but preserves its typical exponential-shape. Adding decoherence to the system gives a far more solid answer to this question. One sees in Fig. 4 that the exponential tail peak is almost completely destroyed after 10 spontaneous emissions on the average (dashed red and cyan dot-dashed lines), which strongly suggested that it is indeed due to interference effects and can thus be attributed to a survival of AL. On the other hand, as expected, the self-trapping regime Fig. 4b is very robust against decoherence.

4 Scaling laws

Sensitivity to the initial conditions is a common feature of nonlinear systems. The nonlinear correction v^{NL} obviously depends on the local density and is therefore highly sensitive to the initial width of the packet: the linear regime is favored for high values of L_0 whereas the chaotic regime and self-trapping regime are expected for spatially concentrated wavepackets. In ref. [15], we showed the existence of scaling laws *on the width L_0 of the initial wavepacket*, which in particular allowed us to classify the three regimes as a function of a *scaled interaction strength* $\tilde{g} = gL_0^{-s}$ with $s = 0.76 \pm 0.08$. Figure 5a, compares the survival function $p(t = 10^5)$ for different values of the initial state width L_0; one clearly sees that the crossovers between the quasilocalised, chaotic and self-trapped regimes indeed strongly depend on L_0. Figure 5b displays the same curves plotted in terms of $\tilde{g}$, showing that the crossovers become independent of the
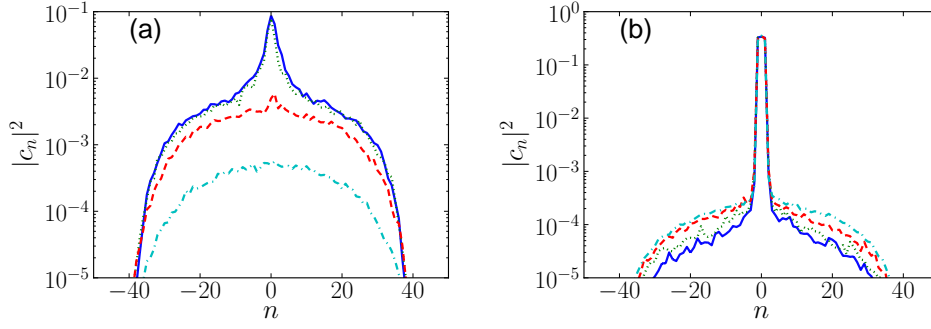
Figure 4. (Color online) Spatial distributions at $t = 10^5$ for $g = 10$(a) and $g = 320$(b), and $\gamma = 0$ (solid blue line), $\gamma = 10^{-5}$ (green dotted), $\gamma = 10^{-4}$ (red dashed) and $\gamma = 10^{-3}$ (dot-dashed cyan). For low nonlinearities and low decoherence levels, Anderson localisation survives for long times, but is finally destroyed by decoherence. The self-trapping regime is almost insensitive to decoherence. Other parameters are $W = 4$, $L_0 = 3$.
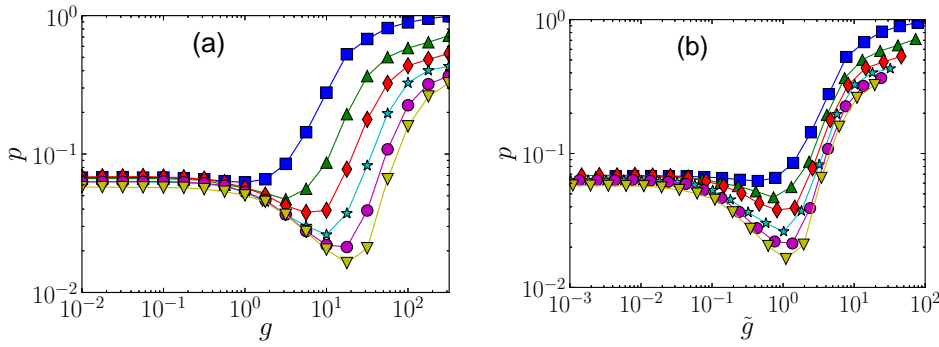

Figure 5. (Color online) Survival probability as a function of the nonlinearity for $W = 1$, $\gamma = 10^{-5}$. (a) No scaling. (b) The scaling in $\tilde{g} = g L_0^{-s}$ ($s = 0.76$) allows a clear identification of regions corresponding to localised ($\tilde{g} < 0.1$), chaotic ($0.1 < \tilde{g} < 10$) and self-trapped ($\tilde{g} > 10$) behaviour. Values of L_0 : 3 (blue squares), 7 (green triangles), 13 (red diamonds), 21 (cyan stars), 31 (magenta circles), 41 (yellow inverted triangles).

initial state, even in the presence of spontaneous emission. As opposed to interactions, decoherence effects are not sensitive to the initial state so it is not surprising that the renormalized nonlinearity remains a "good" parameter.

Figure 6 shows that the probability $p(t)$ can also be approximately scaled in L_0, but the scaling depends on the dynamical regime: $\tilde{p} = p L_0^{\nu}$ with $\nu = 0.52$ in the chaotic regime and $\nu = 0.31$ in the self-trapped regime (and, trivially, $\nu = 0$ in the quasilocalised regime).

5 Conclusion

We have thus characterised the influence of decoherence on the dynamics of interacting bosons in a disordered potential. Spontaneous emission changes considerably the time behaviour of the survival probability, but the use of the scaled parameter $\tilde{g}$ takes into account the crucial sensitivity of the system to the initial conditions, even in presence of decoherence induced by spontaneous emission, allowing a global characterisation of the dynamics. This shows that the effects of interactions and decoherence tend to add up rather than compete. These above results put into evidence the usefullness of
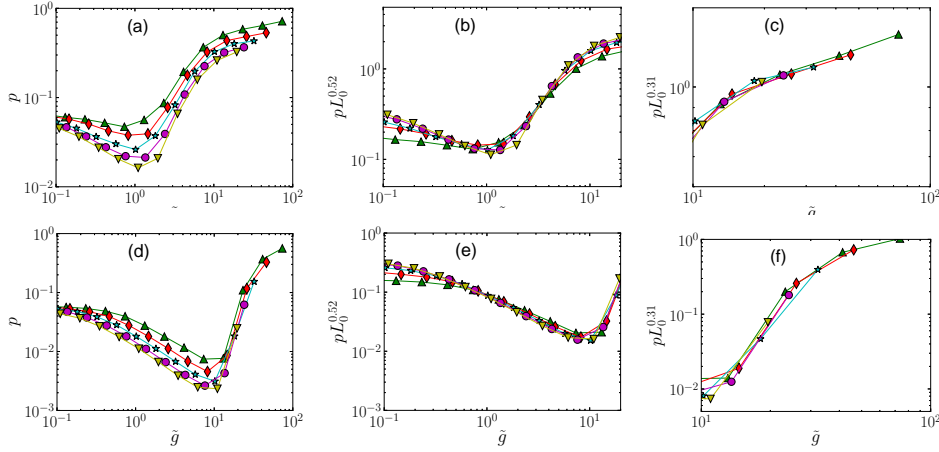
Figure 6. (Color online) Scaling of the survival probability $p(t = 10^5)$ (log-log plot) as a function of the scaled nonlinearity $\tilde{g}$. (a-c) $\gamma = 10^{-5}$ and $W = 4$, (d-f) $\gamma = 10^{-3}$, $W = 1$. Left column: p not scaled and full range in $\tilde{g}$; middle column: p scaled in $L_0^{0.52}$ zoomed on the chaotic region $0.1 \leq \tilde{g} \leq 10$; right column: p scaled in $L_0^{0.31}$ zoomed on the self-trapping region $\tilde{g} > 10$. Values of L_0 : 7 (green triangles), 13 (red diamonds), 21 (cyan stars), 31 (magenta circles), 41 (yellow inverted triangles).

the scaling on the initial state as a tool allowing state independent characterisation of the dynamics, which thus constitutes an important element of a "new language" better adapted to describe the quantum mechanics of nonlinear systems.

References

1. P. W. Anderson. Absence of Diffusion in Certain Random Lattices. *Phys. Rev.*, 109(5):1492–1505, 1958.
2. J. Billy, V. Josse, Z. Zuo, A. Bernard, B. Hambrecht, P. Lugan, D. Clément, L. Sanchez-Palencia, P. Bouyer, and A. Aspect. Direct observation of Anderson localization of matter-waves in a controlled disorder. *Nature (London)*, 453:891–894, 2008.
3. B. Deissler, M. Zaccanti, G. Roati, C. d'Errico, M. Fattori, M. Modugno, G. Modugno, and M. Inguscio. Delocalization of a disordered bosonic system by repulsive interactions. *Nat. Phys.*, 6:354–358, 2010.
4. S. S. Kondov, W. R. McGehee, J. J. Zirbel, and B. DeMarco. Three-Dimensional Anderson Localization of Ultracold Matter. *Science*, 334(6052):66 –68, 2011.
5. F. Jendrzejewski, A. Bernard, K. Muller, P. Cheinet, V. Josse, M. Piraud, L. Pezze, L. Sanchez-Palencia, A. Aspect, and P. Bouyer. Three-dimensional localization of ultracold atoms in an optical disordered potential. *Nat. Phys.*, 8(5):398–403, 2012.
6. F. L. Moore, J. C. Robinson, C. F. Bharucha, B. Sundaram, and M. G. Raizen. Atom Optics Realization of the Quantum δ-Kicked Rotor. *Phys. Rev. Lett.*, 75(25):4598–4601, 1995.
7. H. Lignier, J. Chabé, D. Delande, J. C. Garreau, and P. Szriftgiser. Reversible Destruction of Dynamical Localization. *Phys. Rev. Lett.*, 95(23):234101, 2005.
8. J. Chabé, H. Lignier, H. Cavalcante, D. Delande, P. Szriftgiser, and J. C. Garreau. Quantum Scaling Laws in the Onset of Dynamical Delocalization. *Phys. Rev. Lett.*, 97(26):264101, 2006.

9. G. Casati, I. Guarneri, and D. L. Shepelyansky. Anderson transition in a one-dimensional system with three incommensurable frequencies. *Phys. Rev. Lett.*, 62(4):345–348, 1989.

10. J. Chabé, G. Lemarié, B. Grémaud, D. Delande, P. Szriftgiser, and J. C. Garreau. Experimental Observation of the Anderson Metal-Insulator Transition with Atomic Matter Waves. *Phys. Rev. Lett.*, 101(25):255702, 2008.

11. G. Lemarié, H. Lignier, D. Delande, P. Szriftgiser, and J. C. Garreau. Critical State of the Anderson Transition: Between a Metal and an Insulator. *Phys. Rev. Lett.*, 105(9):090601, 2010.

12. M. Lopez, J.-F. Clément, P. Szriftgiser, J. C. Garreau, and D. Delande. Experimental Test of Universality of the Anderson Transition. *Phys. Rev. Lett.*, 108(9):095701, 2012.

13. G. Lemarié, J. Chabé, P. Szriftgiser, J. C. Garreau, B. Grémaud, and D. Delande. Observation of the Anderson metal-insulator transition with atomic matter waves: Theory and experiment. *Phys. Rev. A*, 80(4):043626, 2009.

14. C. Chin, R. Grimm, P. Julienne, and E. Tiesinga. Feshbach resonances in ultracold gases. *Rev. Mod. Phys.*, 82(2):1225–1286, 2010.

15. B. Vermersch and J. C. Garreau. Interacting ultracold bosons in disordered lattices: Sensitivity of the dynamics to the initial state. *Phys. Rev. E*, 85(4):046213, 2012.

16. A. S. Pikovsky and D. L. Shepelyansky. Destruction of Anderson Localization by a Weak Nonlinearity. *Phys. Rev. Lett.*, 100(9):094101, 2008.

17. T. V. Laptyeva, J. D. Bodyfelt, D. O. Krimer, C. Skokos, and S. Flach. The crossover from strong to weak chaos for nonlinear waves in disordered systems. *EPL (Europhysics Letters)*, 91(3):30001, 2010.

18. D. Cohen. Quantum chaos, dynamical correlations, and the effect of noise on localization. *Phys. Rev. A*, 44:2292–2313, 1991.

19. M. Lepers, V. Zehnlé, and J. C. Garreau. Suppression of decoherence-induced diffusion in the quantum kicked rotor. *Phys. Rev. A*, 81(6):062132, 2010.

20. J. M. Luck. *Systèmes désordonnés unidimensionnels*. Aléa Sacaly, Gif sur Yvette, France, 1992.